Theoretical Study on the Kinetics and Mechanism for the Reaction of FCO with NO†

Kun Xu,‡ Zhen-Feng Xu, and M. C. Lin*

Department of Chemistry, Emory University, Atlanta, Georgia 30322

Received: October 29, 2005; In Final Form: January 20, 2006

The radical reaction mechanism of FCO + NO on the ground electronic state energy surface has been studied at the G2M level of theory based on the geometric parameters optimized at the B3LYP/6-311+G(d) level of theory. The two kinds of reaction pathways include the direct fluorine abstraction channel producing CO + FNO and the association channel forming the FC(O)NO complex. The former has a distinct barrier of 8.9 kcal mol^{-1}, while the latter is a barrierless association process. The rate constant of this reaction system in the temperature range 200−3000 K has been calculated by the microcanonical VTST/RRKM theory. The theoretical result shows that the predicted total rate constants exhibit a negative-temperature dependence and positive-pressure effect at lower temperatures. Under the experimental conditions, the predicted values are in good agreement with the experimental results. In addition, the predicted branching ratios clearly indicate that the dominant product channel is the formation of FC(O)NO at low temperatures and FNO + CO at high temperatures (>500 K).

Introduction

The reaction of FCO radical with NO plays an important role in the atmospheric chemistry of the radical. There have been three experimental studies referring to this reaction in the recent decade. The earliest experiment was carried out by pulse-radiolysis/transient UV absorption spectroscopy in 1994 by Wallington et al.[1] They obtained the rate constant for FCO + NO, $k = (1.0 \pm 0.2) \times 10^{-12}$ cm^3 $molecule^{-1}$ s^{-1}, at 296 ± 2 K and 750 Torr SF_6 pressure. In the following year, Behr, Shafranovsky, and Heydtmann[2] reported the rate constant $k = (5.7^{+1.8}_{-0.9}) \times 10^{-14}$ cm^3 $molecule^{-1}$ s^{-1} at 298 K in 2.3 Torr He using a discharge flow reactor with mass spectrometry. More recently, Ninomiya et al.[3] measured the rate constant by cavity ring-down/UV absorption spectroscopy at 295 K with $k = (1.76 \pm 0.11) \times 10^{-13}$ and $(2.37 \pm 0.21) \times 10^{-13}$ cm^3 $molecule^{-1}$ s^{-1} at 4.0 and 7.0 Torr N_2 pressure, respectively. They also attempted to extrapolate the low (k^0) and high (k^∞) pressure limit rate constants by Troe's formulation and obtained $(2.4 \pm 0.2) \times 10^{-30}$ cm^6 $molecule^{-2}$ s^{-1} and $(1.0 \pm 0.2) \times 10^{-12}$ cm^3 $molecule^{-1}$ s^{-1}, respectively.

Two theoretical papers on the mechanism of this reaction were published in 1998 and 1999, respectively. The earlier paper by Kulkarni and Koga[4] reported a reaction channel via a complex FC(O)NO and a transition state to FNO + CO, calculated at the B3LYP/6-311G(d) and MP2/6-31+(d) levels of theory. The later paper reported two reaction channels calculated at the B3LYP/6-311+G(3df) and CCSD(T)/6-311G-(2d) methods by Liu and Francisco.[5] One of the two channels in Liu and Francisco's paper is essentially consistent with Kulkarni and Koga's, and the other new channel is a direct abstraction of the fluorine atom from FCO by NO to yield FNO and CO.

In view of the above rather limited studies and the apparent absence of any attempt to compare predicted rate constants and product branching ratios as functions of temperature and pressure, we have taken up a more detailed ab initio kinetic study on this reaction system to fully elucidate the mechanism. In the study, the computed potential energy surfaces (PESs) and associated transition state parameters have been utilized to compute the theoretical rate constants for comparison with the available experimental data.

The results of this detailed study are reported herein.

Computational Methods

Geometric parameters of the reactants, products, transition states, and intermediates are optimized at the spin unrestricted B3LYP density functional theory[6] with the 6-311+G(d) basis set. All the stationary points have been identified for local minima and transition states by vibrational analysis, and the unscaled vibrational frequencies are employed for the calculation of zero-point energy (ZPE) corrections, the characterization of stationary points, and rate constant calculations. For a more accurate evaluation of the energetic parameters, higher-level single-point energy calculations of the stationary points were carried out by the modified Gaussian-2 (G2M) theory,[7] based on the optimized geometries at the B3LYP/6-311+G(d) level of theory. The G2M(CC2) method calculates the base energy at the PMP4/6-311G(d) level of theory and improves it with the expanded basis set and coupled-cluster corrections as well as a "higher-level correction (HLC)". All electronic structure calculations were performed with the GAUSSIAN 98 program.[8]

The rate constant for the barrierless association reaction producing FC(O)NO was calculated by the VARIFLEX code[9] based on the microcanonical variational transition state and Rice−Ramsperger−Kassel−Marcus (RRKM) theory.[10] The component rates were evaluated at the *E*/*J*-resolved level, and the pressure dependence was treated by one-dimensional (1D) master equation calculations using the Boltzmann probability of the complex for the *J* distribution. For the barrierless association/decomposition process, the fitted Morse function, $V(R) = D_e\{1 - \exp[-\beta(R - R_e)]\}^2$, was used to represent the minimum potential energy path (MEP) as will be discussed later. Here, D_e is the bonding energy excluding zero-point vibrational

† Part of the special issue "David M. Golden Festschrift".

* To whom correspondence should be addressed. E-mail: chemmcl@emory.edu.

‡ Undergraduate student at the Georgia Institute of Technology.

10.1021/jp056241g CCC: $33.50
Published on Web 03/04/2006

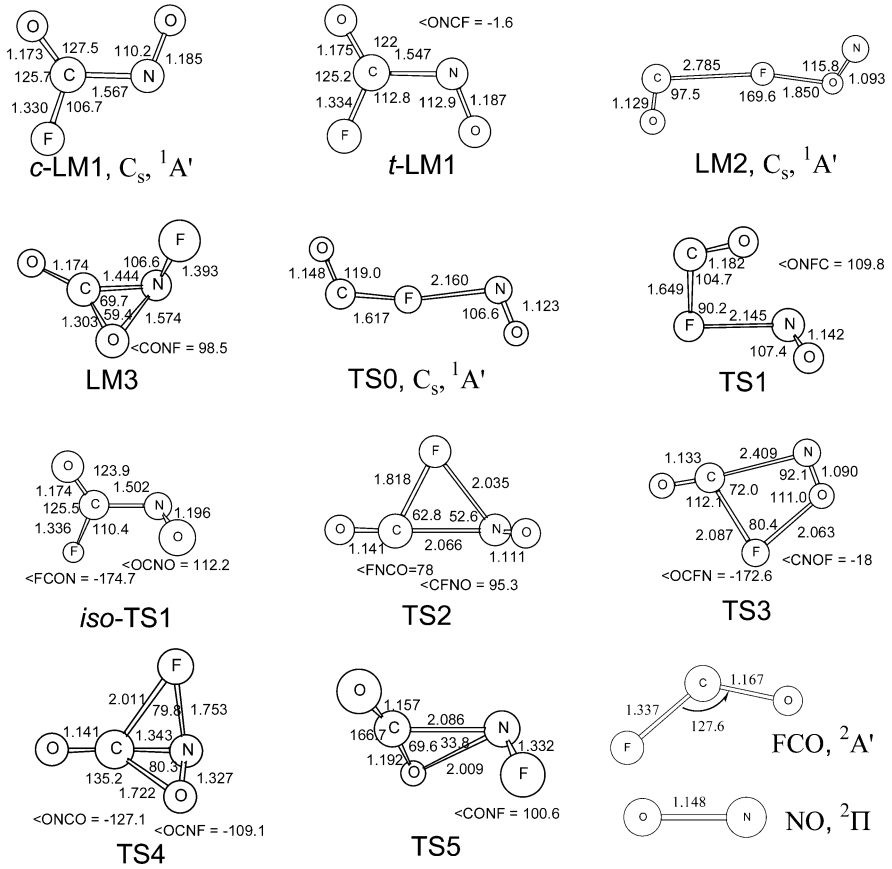

Figure 1. Geometric parameters of the transition states and local minima (length in Å and angle in degrees) on the singlet state PES optimized at the B3LYP/6-311+G(d) level of theory.

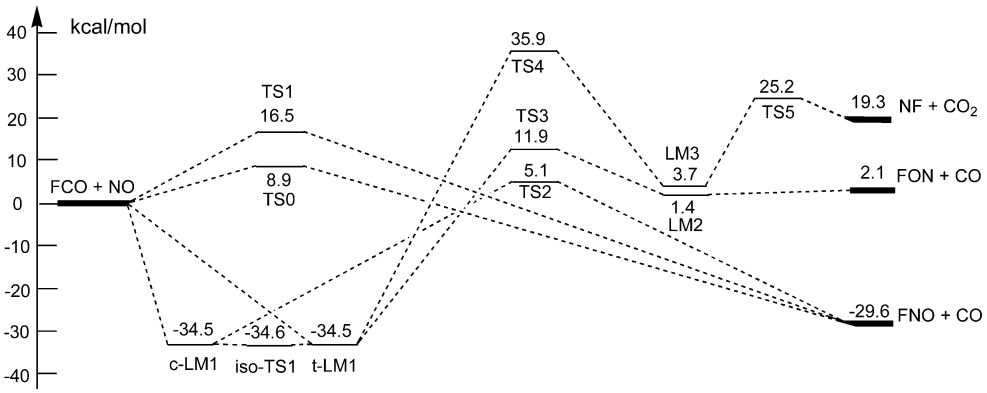

Figure 2. Schematic energy diagram on the singlet state PES predicted at the G2M theory: E(G2M, NO) = −129.743962 au, E(G2M, FCO) = −212.870374 au.

energy for an association reaction, R is the reaction coordinate (i.e., the distance between the two bonding atoms), and R_e is the equilibrium value of R at the stable intermediate structure.

Results and Discussion

Singlet Electronic State Potential Energy Surface. The optimized geometric paremters of the transition states and intermediate complexes are displayed in Figure 1, and the singlet state potential energy surface at the G2M level of theory is presented in Figure 2. The vibrational frequencies and moments of inertia for all the reactants, products, intermediate complexes, and transition states optimized at the B3LYP/6-311+G(d) level of theory are listed in Table 1.

Direct Abstraction Process. From Figure 2, it can be seen that there are two direct fluorine abstraction channels to produce the products FNO and CO. The first channel has a potential barrier of 8.9 kcal/mol via the transition state TS0, which was predicted to be a planar structure, as seen in Figure 1. At this transition state, the breaking bond (C−F) is 1.617 Å, the forming bond (N−F) is 2.160 Å, and the angle of the three atoms (C−F−N) is 169.0°, almost in linearity. It is approximately seen as a trans structure. Table 1 shows that TS0 has only one imaginary vibrational frequency of *i*528 cm^{-1}, whose vibrational vector corresponds to the fluorine-abstraction motion. The second direct fluorine abstraction channel is via TS1 with a potential barrier of 16.5 kcal/mol, which is almost two times greater than that of the first channel. The lengths of breaking bond (C−F) and forming bond (N−F) at TS1 are 1.649 and 2.145 Å, respectively, similar to TS0. But, the angle of C−F−N is 90.2°, considerably different from that of TS0. These geometric parameters and the potential barrier of TS1 are basically consistent with Liu and Francisco's results.[5]

TABLE 1: Vibrational Frequencies and Moments of Inertia for Reactants, Intermediates, Transition States, and Products Predicted at the B3LYP/6-311+G(d) Level of Theory

species	I_i (au)	frequencies (cm^{-1})
FCO	9.6, 157.9, 167.5	626, 1005,1925
NO	35.1, 35.1	1980
CO	31.1, 31.1	2212
FNO	18.9, 155.9, 174.8	498, 766, 1964
CO_2	153.9, 153.9	668, 668, 1372
FON	18.2, 200.1, 218.3	366, 550, 2173
NF	49.1, 49.1	1184
c-LM1	159.2, 396.2, 555.5	40, 294, 407, 537, 697. 771, 1132, 1703, 1933
t-LM1	163.4, 372.2, 535.6	58, 296, 439, 556, 697, 761, 1122, 1690, 1924
LM2	47.2, 1337.8, 1385.0	20, 27, 35, 62, 117, 365, 545, 2177, 2200
LM3	150.6, 374.7, 470.4	238, 417, 529, 632, 749, 865, 939, 1164, 2056
TS0	44.3, 1024.2, 1068.6	*i*528, 18, 81, 153, 170, 360, 496, 1985, 2032
TS1	181.1, 424.3, 564.7	*i*429, 164, 194, 253, 348, 437, 583, 1774, 2119
iso-TS1	177.3, 375.4, 512.7	*i*52, 281, 372, 490, 731, 882, 1106, 1655, 1928
TS2	158.0, 542.6, 662.3	*i*417, 137, 217, 288, 384, 532, 569, 2048, 2088
TS3	186.5, 545.4, 726.7	*i*287, 120, 158, 201, 339, 411, 489, 2159, 2199
TS4	221, 306, 469.0	*i*629, 138, 352, 398, 484, 581, 1039, 1206, 2258
TS5	153.1, 509.6, 597.3	*i*291, 134, 222, 303, 570, 661, 1074, 1286 2304

Association/Dissociation Processes. It is apparent that FCO and NO associate easily through the C−N association to form two isomeric complexes, *cis*-FC(O)NO and *trans*-FC(O)NO (denoted by c-LM1 and t-LM1, respectively). The C−N lengths of c-LM1 and t-LM1 are predicted to be 1.567 and 1.547 Å, respectively, close to the single bond length, 1.474 Å, of the H_3C-NH_2 molecule.[11] Both isomers lie below the reactants by 34.5 kcal/mol at the G2M level. The isomerization transition state (iso-TS1) between c-LM1 and t-LM1 was determined at the B3LYP/6-311+G(d) level of theory, and its energy is only 0.4 kcal/mol higher than that of LM1. With the G2M correction, iso-TS1 is lower than LM1s by 0.1 kcal/mol. This means both isomers can be readily transformed to each other with almost no energy barrier, which is similar to the case of the HCO + NO reaction reported in our previous paper.[12]

In addition, the complexes, c-LM1 and t-LM1, can further dissociate and isomerize. From c-LM1, the dissociation takes place to the products, FNO + CO, via the transition state, TS2, which is 5.1 kcal/mol higher than reactants at the G2M level. TS2 is a trianglular structure, in which the forming F−N bond is 2.035 Å and both the breaking C−F and C−N bonds are 1.818 and 2.066 Å, respectively, at the B3LYP/6-311+G(d) level of theory. These geometric parameters of TS2 are essentially consistent with those optimized by Kulkarni and Koga[4] and Liu and Francisco.[5]

From t-LM1, there are two sub-channels to products, FON + CO and NF + CO_2. The FON + CO producing process proceeds via a four-membered ring transition state, TS3, and a complex, LM2. At TS3, the lengths of the breaking bonds F−C and N−C are 2.087 and 2.409 Å, respectively, and that of the forming bond F−O is 2.065 Å. At LM2, the breaking bond F−C elongates to 2.785 Å, almost completely broken. The G2M energies of TS3 and LM2 relative to that of the reactants are predicted to be 11.9 and 3.7 kcal/mol, respectively. Apparently, LM2 can readily decompose to produce FON and CO because of the small energy difference of only 0.7 kcal/mol between LM2 and FON + CO. Another sub-channel to produce NF + CO_2 contains two transition states (TS4 and TS5) and a complex (LM3). From Figure 2, one can see that TS4 was predicted to have a high energy of 35.9 kcal/mol, which is the highest barrier in this reaction system. LM3 is 3.7 kcal/mol higher than the reactants and can further decompose to products NF + CO_2 via TS5. However, this sub-channel obviously cannot compete with the above processes kinetically.

Rate Constant Calculations. The rate constants for the direct fluorine abstraction were calculated by the conventional transition state theory and that for the barrierless association and dissociation computed by the variational RRKM rate theory. The temperature dependence was studied in the temperature range 200−3000 K. The pressure-dependent rate constant for the association channel was evaluated at the *E*/*J*-resolved level by solving the 1D master equation. To achieve convergence in the integration over the energy range from 12 000 cm^{-1} below to 68 000 cm^{-1} above the threshold, an energy grain size of 100 cm^{-1} was used for the temperature range 200−3000 K. The total angular momentum *J* covered the range from 1 to 241 in step of 10 for the *E*/*J*-resolved calculation. Helium, nitrogen, and SF_6 were employed as buffer gases with the average energies of 100, 200, and 400 cm^{-1}, respectively, transferred per collision, and their Lennard-Jones (L-J) parameters were taken from the literature.[13] For the prediction of the quenching rates, the L-J parameters of the complex were taken to be approximately $\epsilon/k = 84.1$ K and $\sigma = 3.26$ Å, the same as those in the HCO + NO reaction system.[12] The barrierless association process, FCO + NO → LM1, was optimized by manually varying the C−N distances point by point with an interval of 0.1 Å from LM1 to the reactants, shown in Figure 3. These association potential energy points were fitted by the Morse function with the expression $V(R) = 37.4 \times \{1 - \exp[-2.186 \times (R - 1.567)]\}^2$, which reasonably represents the corresponding association minimum energy path.

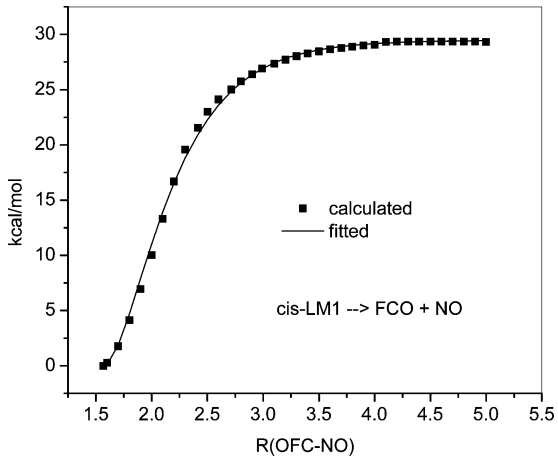

Figure 3. Morse curve for the dissociation reaction c-LM1 → FCO + NO.

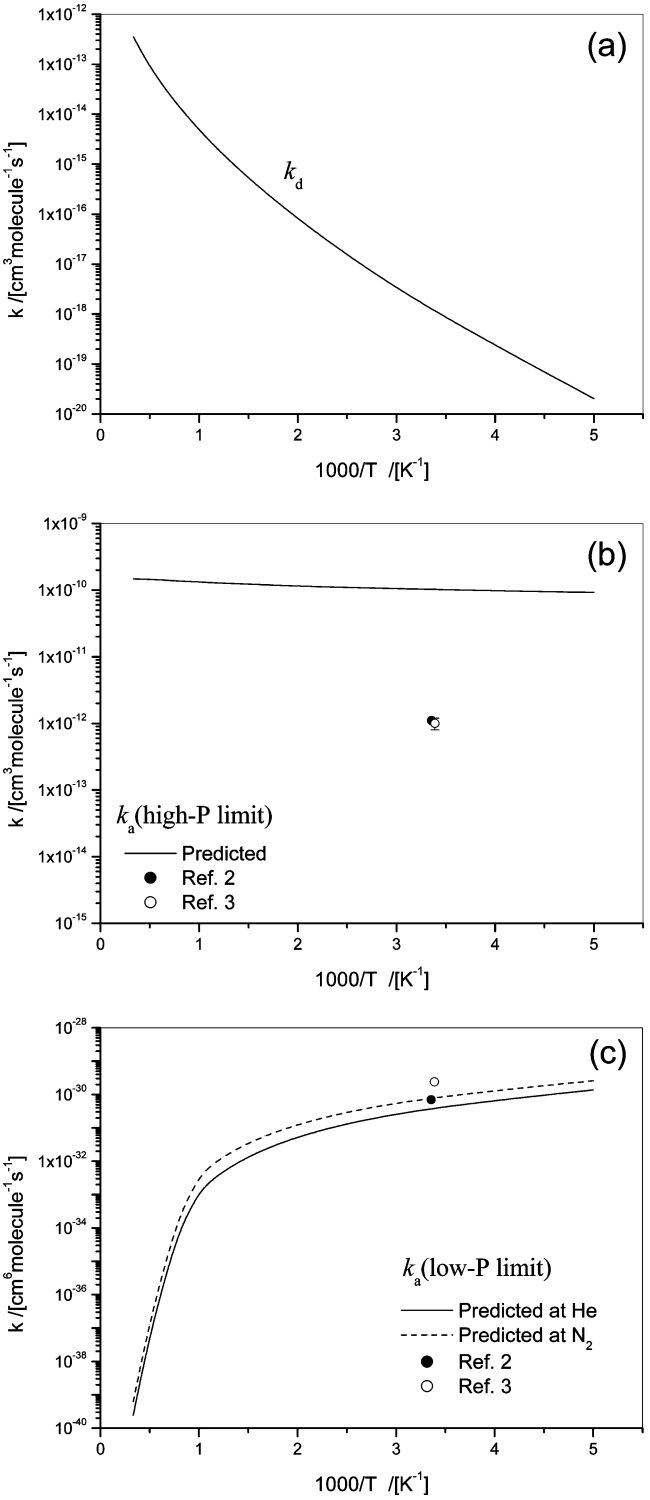

Figure 4. Rate constant plots of (a) fluorine direct abstraction channel FCO + NO → (TS0) → FNO + CO, (b) association channel FCO + NO → LM1 at infinite pressure, and (c) association channel FCO + NO → LM1 in He and N_2 .

The predicted rate constant (k_d) for the production of FNO + CO via TS0 is plotted in Figure 4a. It should be mentioned that the torsional vibration of TS0 with a low frequency of 18 cm^{-1} was treated as the free internal rotation around the N−F axis with the rotational constant of 2.692 cm^{-1}. Because of this, the rate constants at 500 and 1000 K decrease 22% and 36%, respectively. The predicted rate constants for the association reaction at the high-pressure (k_a^∞) and low-pressure (k_a^0) limits are displayed in parts b and c of Figure 4, respectively. These data can be represented in the temperature range 200−3000 K by the following expressions

$$k_d = 3.27 \times 10^{-20} T^{2.74} \exp(-4282/T) \text{ cm}^3 \text{ molecule}^{-1} \text{ s}^{-1}$$

$$k_a^\infty = 6.34 \times 10^{-11} T^{0.112} \exp(-45.6T) \text{ cm}^3 \text{ molecule}^{-1} \text{ s}^{-1}$$

$$k_a^0(\text{He}) = 9.34 \times 10^{-13} T^{-6.80} \exp(-1010/T) \text{ cm}^6 \text{ molecule}^{-2} \text{ s}^{-1} \quad (200-1000 \text{ K})$$

$$= 1.58 \times 10^6 T^{-13.27} \exp(1806/T) \text{ cm}^6 \text{ molecule}^{-2} \text{ s}^{-1} \quad (1000-3000 \text{ K})$$

$$k_a^0(\text{N}_2) = 2.64 \times 10^{-13} T^{-6.47} \exp(-987/T) \text{ cm}^6 \text{ molecule}^{-2} \text{ s}^{-1} \quad (200-1000 \text{ K})$$

$$= 7.37 \times 10^5 T^{-13.08} \exp(2327/T) \text{ cm}^6 \text{ molecule}^{-2} \text{ s}^{-1} \quad (1000-3000 \text{ K})$$

$$k_a^0(\text{SF}_6) = 3.46 \times 10^{-14} T^{-6.02} \exp(-942/T) \text{ cm}^6 \text{ molecule}^{-2} \text{ s}^{-1} \quad (200-1000 \text{ K})$$

$$= 4.52 \times 10^3 T^{-12.42} \exp(3899/T) \text{ cm}^6 \text{ molecule}^{-2} \text{ s}^{-1} \quad (1000-3000 \text{ K})$$

The total rate constants predicted for various pressures between 1 and 760 Torr, including those employed in previous experiments, within the temperature range 200−3000 K are presented in Figure 5. Apparently, the total rate constants are positively P-dependent and negatively T-dependent at lower temperatures. With the temperature increasing beyond 500 K, the rate constants rise rapidly because of the increasing contribution form the F-abstraction process which has a positive-T dependence. In addition, for the predicted rate constants at 2.3 Torr He and at 4.0 and 7.0 Torr N_2, the agreement between theory and experiment is seen to be quite good. The reported P-dependence for the N_2 buffer gas at room temperature could be reasonably accounted for as also shown in Figure 6. However, the predicted rate constant at 750 Torr SF_6 pressure is about 24 times greater than the experimental value obtained by pulsed-radiolysis/UV absorption spectrometry.[1] In view of the close agreement between theory and experiment with He and N_2 diluents and the fact that the 750 Torr SF_6 result is only 4 times larger than that of the 7 Torr N_2 value measured at room temperature, a new determination for the former condition should be made to help resolve the difference. It should be noted that our previous studies on a variety of barrierless association processes, such as $CH_3 + O_2$,[14] $ClO + NO_2$,[15] $CH_3 + C_2H_5$,[16] $HO_2 + NO$,[17] and the unimolecular decomposition of $HOClO_3$,[18] among others, by means of the G2M-VRRKM calculations over a wide range of P and T conditions led to very good agreement between theory and experiment.

The predicted association rate constant in the high-pressure limit as shown in Figure 4b is about 2 orders of magnitude higher than the extrapolated values at 298 K given in ref 2 and 295 K in ref 3. Also, the association rate constant predicted for the low-pressure limit is about 1.6 times smaller than the extrapolated value for He[2] and 2.9 times smaller than that for N_2.[3] The deviations, particularly that for the high-P limit,

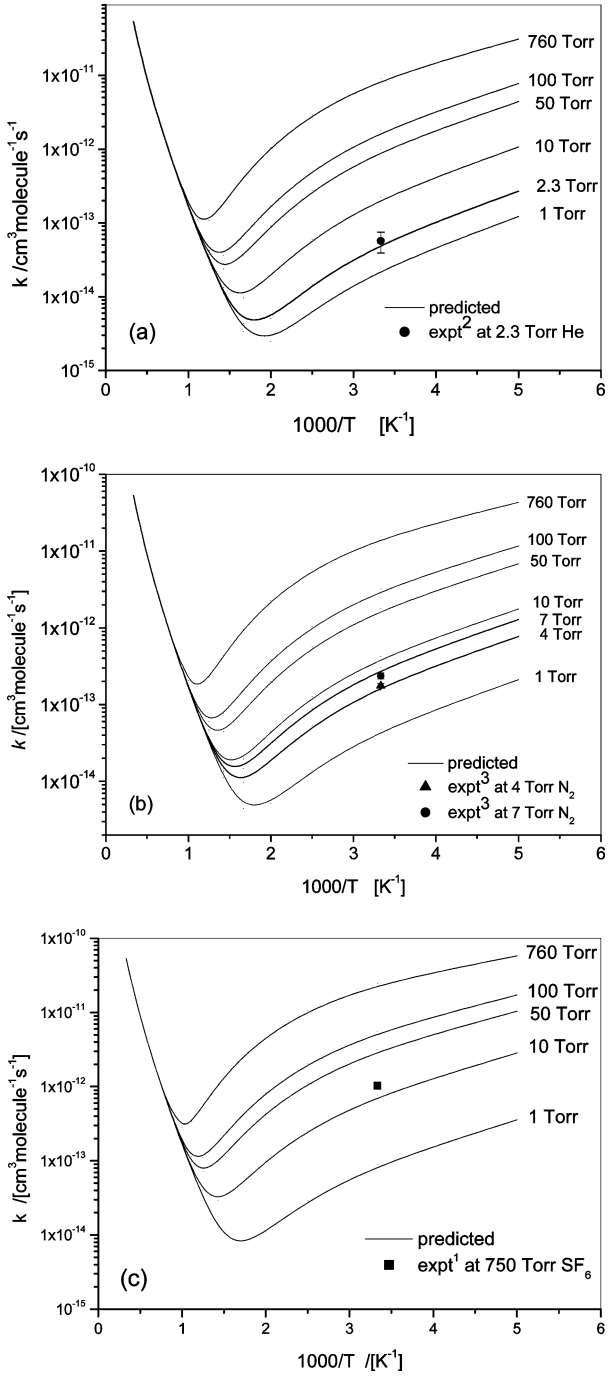

Figure 5. Comparison of the predicted total rate constants (k_{total}) with the experimental data in (a) He, (b) N_2, and (c) SF_6 buffer gases.

obviously result from the unreliably long extrapolation of limited P-dependent data obtained at $P < P_{1/2}$ at which $k_p/k^\infty = {}^1/_2$. k_p measured at $P < P_{1/2}$ does not contain sufficient transition state information for that process. Figure 6 clearly illustrates the danger of such a long extrapolation based on a scarce number of rate coefficients in a limited pressure range.

Figure 7 shows the product branching ratios of LM1, FNO, and FON at 10 Torr He pressure from 200 to 3000 K. Apparently, the complex intermediate LM1 is the dominant product under about 400 K and FNO + CO becomes the main product over about 900 K. From 400 to 900 K, the branching ratio of LM1 decreases rapidly while the branching ratio of FNO increases steeply. At about 640 K, the branching ratio of LM1 and FNO is about 0.5 each. In the whole temperature regime, the branching ratio of FON is very small, and its maximum

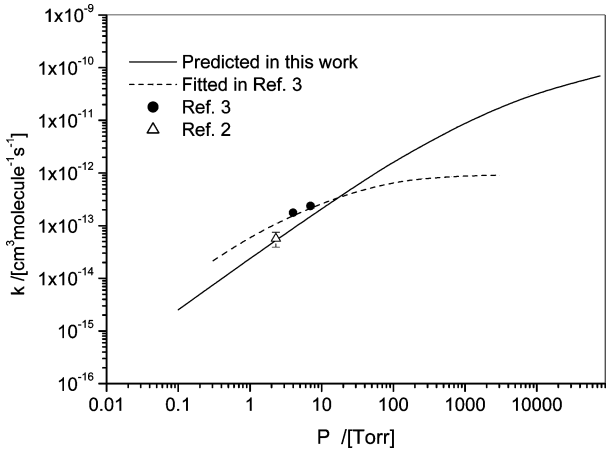

Figure 6. Rate constant vs N_2 buffer gas pressure at 298 K.

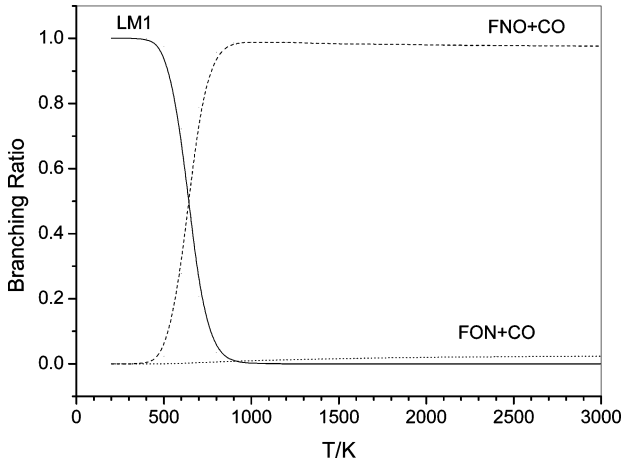

Figure 7. Branching ratios for the formation of FNO, FON, and LM1 at 10 Torr He as functions of temperature.

value does not exceed 0.025. Therefore, with the temperature variation from low to high, the dominant product changes from LM1 to FNO + CO.

Conclusions

The mechanism for the FCO + NO reaction on the ground electronic state energy surface has been studied at the G2M//B3LYP/6-311+G(d) level of theory. Two distinct reaction pathways have been confirmed. One is the direct fluorine abstraction reaction producing CO + FNO, and the other is the association reaction forming FC(O)NO complexes. The abstraction reaction can take place via two different transition states, having C_s and C_1 symmetries, with 8.9 and 16.5 kcal/mol barriers, respectively. The second path is a barrierless association process forming the FC(O)NO complexes with *cis*- and *trans*-OCNO structures, both lie 34.5 kcal/mol below the reactants. Further decomposition of the cis- and trans-complexes to give FNO + CO and FON + CO, respectively, can occur with 5.1 and 11.9 kcal/mol barriers. These product formation channels are unimportant at temperatures below 500 K under experimental conditions. The rate constants calculated by the microcanonical VTST/RRKM theory in the temperature range 200−3000 K show that the total rate constants have a negative temperature dependence and positive-pressure effect in the lower temperature regime; the predicted values are in good agreement with the experimental results with He and N_2 as buffer gases. However, theory over-predicted the rate constant with SF_6 as the diluent. Under experimental conditions, the predicted

branching ratios clearly indicate that the dominant products are FC(O)NO complexes at lower temperatures and FNO + CO at higher temperatures (>500 K).

Acknowledgment. We gratefully acknowledge the supports from the Basic Energy Sciences, Department of Energy, under Contract No. DE-FG02-97-ER14784, and from an ONR-SBIR project through Contract No. N00014-02-C-0292 (to Z.F.X.). M.C.L. acknowledges the support from the Taiwan National Science Council for a Distinguished Visiting Professorship at the Center for Interdisciplinary Molecular Science, Chiao Tung University, Hsinchu, Taiwan.

References and Notes

(1) Wallington, T. J.; Ellermann, T.; Nielsen, O. J.; Sehested, J. *J. Phys. Chem.* **1994**, *98*, 2346.

(2) Behr, P.; Shafranovsky, E.; Heydtmann, H. *Chem. Phys. Lett.* **1995**, *247*, 327.

(3) Ninomiya, Y.; Goto, M.; Hashimoto, S.; Kawasaki, M.; Wallington, T. J. *Int. J. Chem. Kinet.* **2001**, *33*, 130.

(4) Kulkarni, S. A.; Koga, N. *J. Phys. Chem. A* **1998**, *102*, 5228.

(5) Liu, R.; Francisco, J. S. *Chem. Phys. Lett.* **1999**, *303*, 664.

(6) (a) Becke, A. D. *J. Chem. Phys.* **1993**, *98*, 5648. (b) Lee, C.; Yang, W.; Parr, R. G. *Phys. Rev. B* **1988**, *37*, 785.

(7) Mebel, A. M.; Morokuma, K.; Lin, M. C. *J. Chem. Phys.* **1995**, *103*, 7414.

(8) Frisch, M. J.; Trucks, G. W.; Schlegel, H. B.; Scuseria, G. E.; Robb, M. A.; Cheeseman, J. R.; Montgomery, J. A., Jr.; Vreven, T.; Kudin, K. N.; Burant, J. C.; Millam, J. M.; Iyengar, S. S.; Tomasi, J.; Barone, V.; Mennucci, B.; Cossi, M.; Scalmani, G.; Rega, N.; Petersson, G. A.; Nakatsuji, H.; Hada, M.; Ehara, M.; Toyota, K.; Fukuda, R.; Hasegawa, J.; Ishida, M.; Nakajima, T.; Honda, Y.; Kitao, O.; Nakai, H.; Klene, M.; Li, X.; Knox, J. E.; Hratchian, H. P.; Cross, J. B.; Adamo, C.; Jaramillo, J.; Gomperts, R.; Stratmann, R. E.; Yazyev, O.; Austin, A. J.; Cammi, R.; Pomelli, C.; Ochterski, J. W.; Ayala, P. Y.; Morokuma, K.; Voth, G. A.; Salvador, P.; Dannenberg, J. J.; Zakrzewski, V. G.; Dapprich, S.; Daniels, A. D.; Strain, M. C.; Farkas, O.; Malick, D. K.; Rabuck, A. D.; Raghavachari, K.; Foresman, J. B.; Ortiz, J. V.; Cui, Q.; Baboul, A. G.; Clifford, S.; Cioslowski, J.; Stefanov, B. B.; Liu, G.; Liashenko, A.; Piskorz, P.; Komaromi, I.; Martin, R. L.; Fox, D. J.; Keith, T.; Al-Laham, M. A.; Peng, C. Y.; Nanayakkara, A.; Challacombe, M.; Gill, P. M. W.; Johnson, B.; Chen, W.; Wong, M. W.; Gonzalez, C.; Pople, J. A. *Gaussian 03*, revision C.01; Gaussian, Inc.: Wallingford, CT, 2004.

(9) Klippenstein, S. J.; Wagner, A. F.; Dunbar, R. C.; Wardlaw, D. M.; Robertson, S. H. *VARIFLEX*, version 1.00, 1999.

(10) (a) Wardlaw, D. M.; Marcus, R. A. *Chem. Phys. Lett.* **1984**, *110*, 230. (b) Wardlaw, D. M.; Marcus, R. A. *J. Chem. Phys.* **1985**, *83*, 3462. (c) Klippenstein, S. J. *J. Chem. Phys.* **1992**, *96*, 367. (d) Klippenstein, S. J.; Marcus, R. A. *J. Chem. Phys.* **1987**, *87*, 3410.

(11) Kennard, O. *CRC Handbook of Chemistry and Physics*, 64th ed.; Weast, R. C., Astle, M. J., Beyer, W. H., Eds.; CRC Press, Inc.: Boca Raton, FL, 1984; p F171.

(12) Xu, Z. F.; Hsu, C.-H.; Lin, M. C. *J. Chem. Phys.* **2005**, *122*, 234308.

(13) Hippler, H.; Troe, J.; Wendelken, H. J. *J. Chem. Phys.* **1983**, *78*, 6709.

(14) Zhu, R. S.; Hsu, C.-C.; Lin, M. C. *J. Chem. Phys.* **2001**, *115*, 195.

(15) Zhu, R. S.; Lin, M. C. *ChemPhysChem* **2005**, *5*, 1864.

(16) Zhu, R. S.; Xu, Z. F.; Lin, M. C. *J. Chem. Phys.* **2004**. *120*, 6566.

(17) Zhu, R. S.; Lin, M. C. *J. Chem. Phys.* **2003**, *119*, 10667.

(18) Zhu, R. S.; Lin, M. C. *PhysChemComm* **2001**, *25*, 1.